Fatigue Life of Resistance Spot Welding on Dual-Phase Steels

J. H. Ordoñez Lara, R. R. Ambriz, C. García, G. Plascencia and D. Jaramillo

Introduction

Dual-phase steels are composed by a ferrite matrix and martensite as second phase. This characteristic allows to obtain an excellent combination of high strength and ductility, which is very attractive for the automotive industry to reduce the total weight of the vehicles. Resistance spot welding (RSW) is commonly used in the automotive industry to join the automobile parts, i.e. a vehicle has around three thousand welding points. However, due to the welding process (heat input), microstructural changes can be induced, which affects the mechanical behavior of the welded joints. In this context, several studies have been carried out [1–4]. Nayak et al. [1] studied the soft zone generated in the heat affected zone (HAZ) in RSW in dual-phase steels. They observed a tempering of the martensite in the HAZ, which affects the tensile properties of the joints. Additionally, Farabi et al. [5] analyzed the microstructure and mechanical properties of dissimilar laser welding in dual-phase steels. It was found that a microstructural change (almost 100% martensite) in the fusion zone (FZ) increases the hardness (50 HV), also they observed that the failure zone after tensile tests was presented in the soft zone formation in the HAZ. In contrast, the fatigue failure was attribute to the stress concentration effect produced by the nugget zone. Mediratta et al. [6] studied the influence of ferrite and martensite microstructure in fatigue life considering low cyclic fatigue. They found that the different microstructure of the material exhibits a cyclic hardening effect. The lower hardening occurs when there is a uniform

J. H. Ordoñez Lara (✉) · R. R. Ambriz · G. Plascencia · D. Jaramillo
Instituto Politécnico Nacional CIITEC-IPN, Cerrada de Cecati S/N,
Col. Sta. Catarina, 02250 Azcapotzalco, Ciudad de México, Mexico
e-mail: pure_evil_h@hotmail.com

C. García
Facultad de Ingeniería, Universidad Autónoma de San Luis Potosí,
Av. Manuel Nava no. 8, Zona Universitaria, 78290 San Luis Potosí, S.L.P., Mexico

distribution of dislocations due to the dispersion of martensite. In contrast, fine grains and continuous martensite around the ferrite grains present the best performance for the fatigue life. Pouranvari [2] performed a study on the susceptibility to interfacial failure in RSW of DP600 dual phase steel. He found a transition from interfacial failure to pullout failure which depends of the size of the melting zone. The high carbon content of the steel promotes the martensite formation, as well as the propagation of cracks through the melting zone. There is no direct correlation between the equivalent carbon and the tendency to interfacial fracture in shear tensile test. Dancette et al. [4] carried out a study on the tensile shear fracture of advanced high-strength steel spot welds. They identified two fracture mechanisms, the first one was related with the localized deformation in the base material, the second one was associated with the ductile shear at the interface of the nugget zone. Giri and Bhattacharjee [7] studied the fatigue life in DP590 steel; they reported that the stress concentration generated in the fusion zone reduces the fatigue life of the welded joints. In contrast, Sherman and Davies [8] conducted a study of the effect of martensite content on fatigue life in dual-phase steels, reporting that the strength of the joints tends to improve when the martensite volume increases.

This work reports a comparative scenario between the DP590 and DP980 steels welded by RSW. The results are reported in terms of microhardness, shear and fatigue tests. The fatigue life of the joints and the analysis of the fracture surface also are reported.

Experimental Procedure

Materials and Welding

DP590 (σ_0 = 362 MPa σ_u = 596 MPa,   and ε = 23.5%),   and   DP980 (σ_0 = 930 MPa σ_u = 1135 MPa, and ε = 11.5%) steel sheets were used (chemical composition shown in Table 1). Conventional techniques of cutting, machining, grinding and mirror polishing were used to obtain metallographic samples of the materials. The grain structure of the materials is presented in Fig. 1. As it can be observed, the microstructure of the DP590 steel presents a lower volume of martensite in comparison to the DP980, also an important difference in terms of grain size was observed. These characteristics provided an important difference in hardness.

Resistance spot welding (RSW) equipment with alternating current was used. A current of 9.5 kA, with a frequency of 60 Hz and force of 40 kN were used to perform RSW lap joint according with the standard dimensions dictated by the AWS D8.9 specification. Uncoated copper electrodes were used during the welding process. Tips of the electrodes were machined to obtain a circular section of 5 mm in diameter with an angle of 120°.

Table 1 Chemical composition of the materials employed (wt%)

	C	Si	Mn	P	S	Cr	Mo	Ni	Al	Cu	Ti	V	Fe
DP590	0.054	0.43	1.95	0.019	0.0057	0.030	0.0022	0.018	0.038	0.021	0.0017	0.0050	97.43
DP980	0.15	0.2	1.5	0.0096	0.0033	0.037	0.013	0.045	0.034	0.0075	0.0012	0.01	97.98
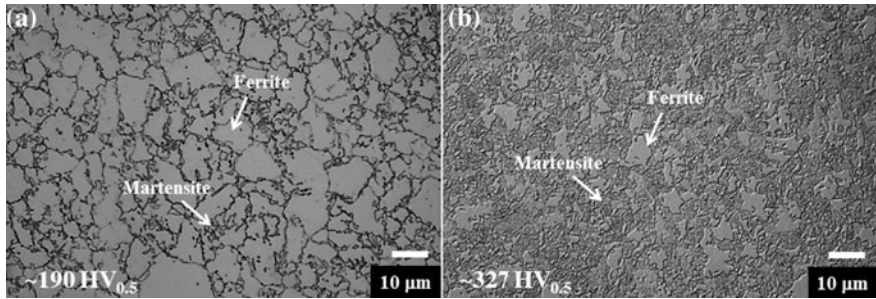
Fig. 1 Dual-phase steel optical microstructure showing a ferrite and martensite phases, **a** DP590 and **b** DP980
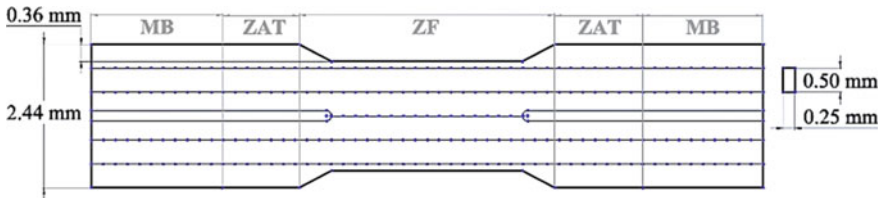
Fig. 2 Schematic welding profile and virtual mesh for microhardness measurements

After welding Vickers microhardness measurements with a load of 0.5 kg and dwell-time of 15 s were taken following the scheme shown in Fig. 2.

Tensile shear tests were performed for the welded joints with head-cross displacement of 0.25 mm min^{-1}. An extensometer with a gage length of 25 mm was used. The specimen dimensions for tensile shear and fatigue tests were 105 mm × 45 mm × 1.22 mm with an overlap of 35 mm. These dimensions were established according with the AWS D8.9 specification. Fatigue tests were performed with a cyclic loading sinusoidal wave form at a stress ratio of $R = 0.1$ by using a frequency of 30 Hz and room temperature (~22 °C). After fatigue tests, some specimens were analyzed by using a scanning electron microscope to observe the fracture surface.

Results and Discussion

Microstructure

Figure 3 shows the macro and microstructure of the cross-section resistance spot welding points obtained. From this figure it is possible to observe the fusion zone (FZ), the heat affected zone (HAZ), and the base material (BM). In both welded
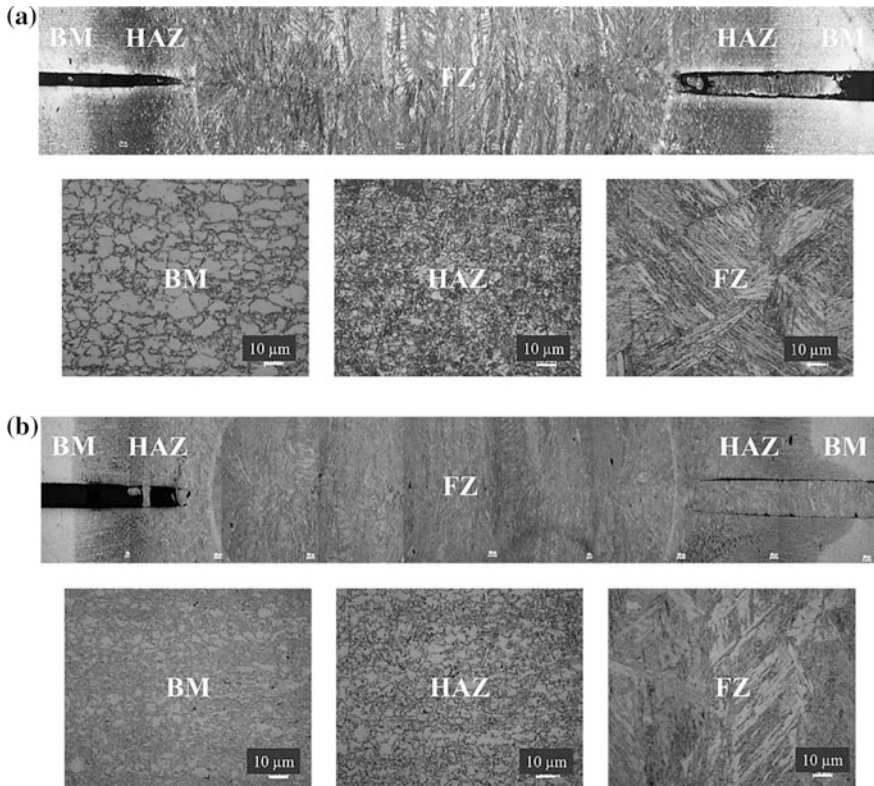
Fig. 3 Microstructure of resistance spot welds **a** DP590 and **b** DP980 steels

joints (DP590 and DP980) the heat input produced during welding produces an evident microstructural change. The FZ is formed by martensite with a lath morphology, which is characteristic for steels with low carbon contents. In the HAZ a grain size refinement was observed with an increment in volume of martensite, especially for the DP980 steel (Fig. 3b).

Microhardness

Figure 4 shows the hardness profile for the DP590 and DP980 spot welds. According to figure it is possible to observe a hardness increment in the center of the FZ, which represents approximately 130 $HV_{0.5}$ and 120 $HV_{0.5}$ for the DP590 and DP980 steels in comparison with the base material hardness. This hardness tends to increase as function of distance from the center of the FZ to the HAZ, reaching values (near to the interface between HAZ and FZ) at about 370 $HV_{0.5}$ and 430 $HV_{0.5}$ for DP590 and DP980 steels, respectively [1]. Considering that the
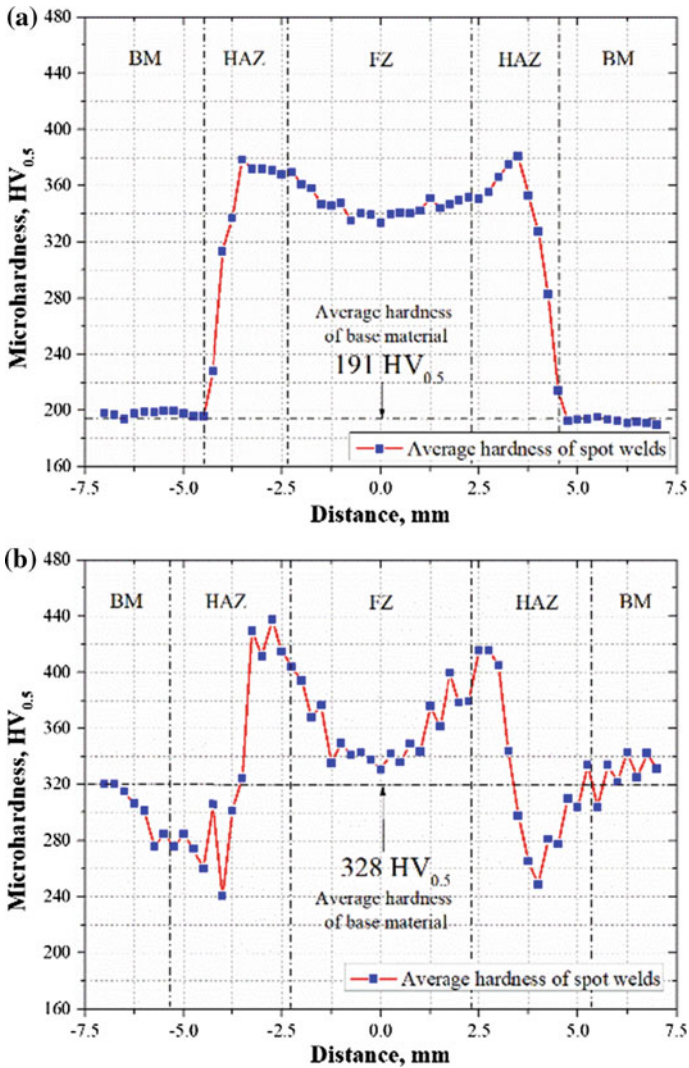
Fig. 4 Microhardness profiles for **a** DP590 and **b** DP980

applied current during welding in both materials is similar, as well as the thermo-physical properties, we can consider that the cooling rate in both materials is also similar. Thus, the increase in hardness on the FZ can be attributed to the chemical composition of the materials [9, 10], as well as the fast cooling rate, i.e. the cooling rate curve traverses the martensitic transformation line of the continuous cooling transformation. Later, a hardness decrement is observed reaching the base material hardness for the DP590 steel. However, in the case of the DP980 steel, a

soft zone formation [5, 11] with hardness values below of that of the base material (320 HV$_{0.5}$) have been observed. This zone was attributed to the weld thermal cycle producing a tempering process (tempered martensite).

Shear Testing

Figure 5 shows the representative (average of three samples) shear load-displacement curves for the DP590 and DP980 steels welded joints. As can be seen, the maximum load is similar in both welded joints ($F_{max} \sim 18$ kN). However, an important difference in terms of displacement was observed for the DP590 (~ 1.73 mm) joints in comparison to the DP980 (~ 0.9 mm) joints. This aspect can be attributed to the microstructural transformation, which tends to increase tensile strength but a decrement in ductility [4, 12, 13] for the DP980 welds. Then, an improvement in fracture energy (fracture toughness) can be deduced for the DP590 welds. In addition, it is possible to note a pullout failure mode after shear testing.
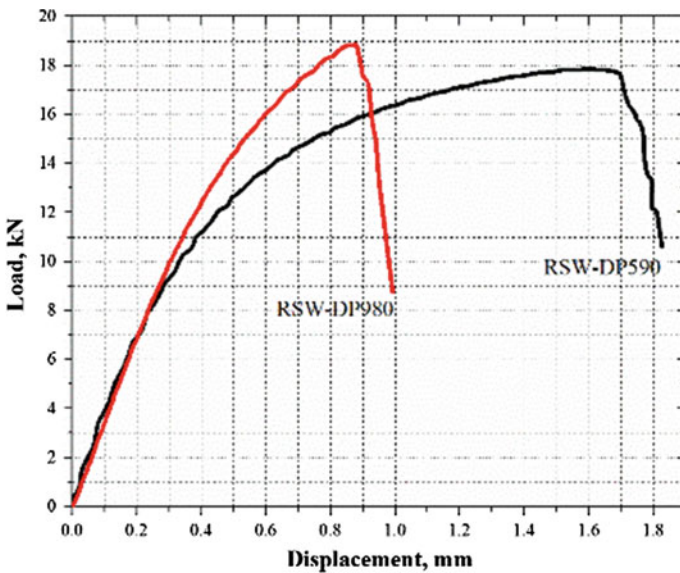

Fig. 5 Shear load-displacement curves for resistance spot welding in DP590 and DP980 steels

Fatigue Behavior (Wöhler Curves)

Resistance spot welds were subjected to a cyclic loading as previously indicated. Figure 6 shows the experimental results obtained for the RSW in DP590 and DP980 steels and its respective comparison with the Wöhler curve found in the literature.
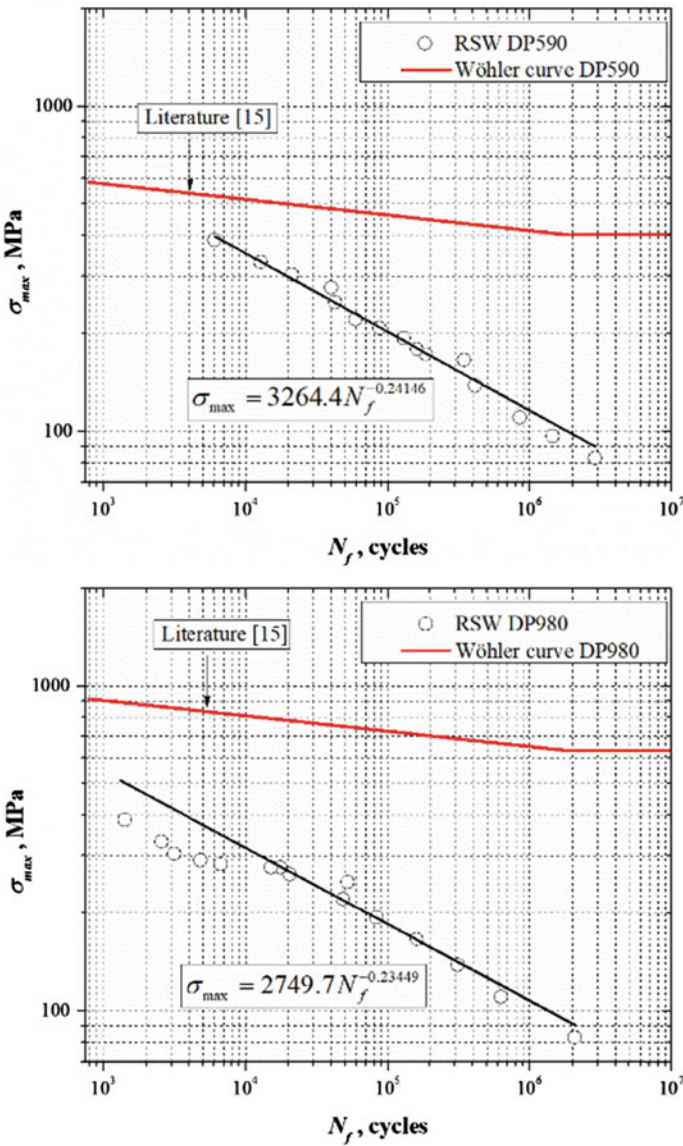

Fig. 6 Experimental Wöhler curves obtained for resistance spot welding in DP590 and DP980 steels and its respective comparison with the base material found in the literature [14]

The experimental data found were fitted to the traditional Basquin's equation:

$$\sigma_{max} = AN_f^b \qquad (1)$$

where A and b are the experimental constants.

Considering the results shown in Fig. 6, it is possible to observe an important effect of the spot welding geometry on the fatigue life with respect to the base material. It is to say that the stress concentration factor is the dominant aspect to decrease the fatigue life of the joints. This aspect was observed in both materials (DP590 and DP980). Thus, it is important to note that the high resistance of the DP980 steel should not be consider as a predominant aspect to design welded structures subjected to cyclic loading. On this context, the authors are carrying out experiments related with overloads to induced compressive residual stresses to improve the fatigue resistance of the RSW in DP980 steel.

In terms of fatigue cracks, it was observed that all the samples tested nucleated the crack at the fusion zone (stress concentration factor), and grew trough the HAZ to the base material, as shown in Fig. 7.

From Fig. 7, two predominant fracture modes can be observed. Mode I from which the crack nucleated and propagates due to the stress concentration produced by the spot welding and the interface between both sheets. Then it changes to Mode III, in which the crack grows throughout the interface between the FZ and the HAZ perpendicular to the applied load across the thickness of the joints [15].

The fracture surface of the joints is shown in Fig. 8. Five sites of the fracture surface were analyzed as indicated by details a1–a5, b1–b5.

The fracture appearance reveals that the crack was nucleated at the interface between sheets (rectangle marked as position 5 in Fig. 8). Later, the crack propagated across the thickness and surface of the sheets in a combination mode I/III. During the propagation of the crack striations were detected, which represents the steps of the cyclic load applied during the fatigue test. On the other hand, microcracks also were observed, which can be attributed to the martensitic microstructure (hard and brittle phase). A larger number of microcracks can be observed in the case of DP980, which can be attributed to the higher volume of martensite, compared to DP590.

Fig. 7 General fatigue fracture appearance for **a** DP590 sample and **b** DP980 sample
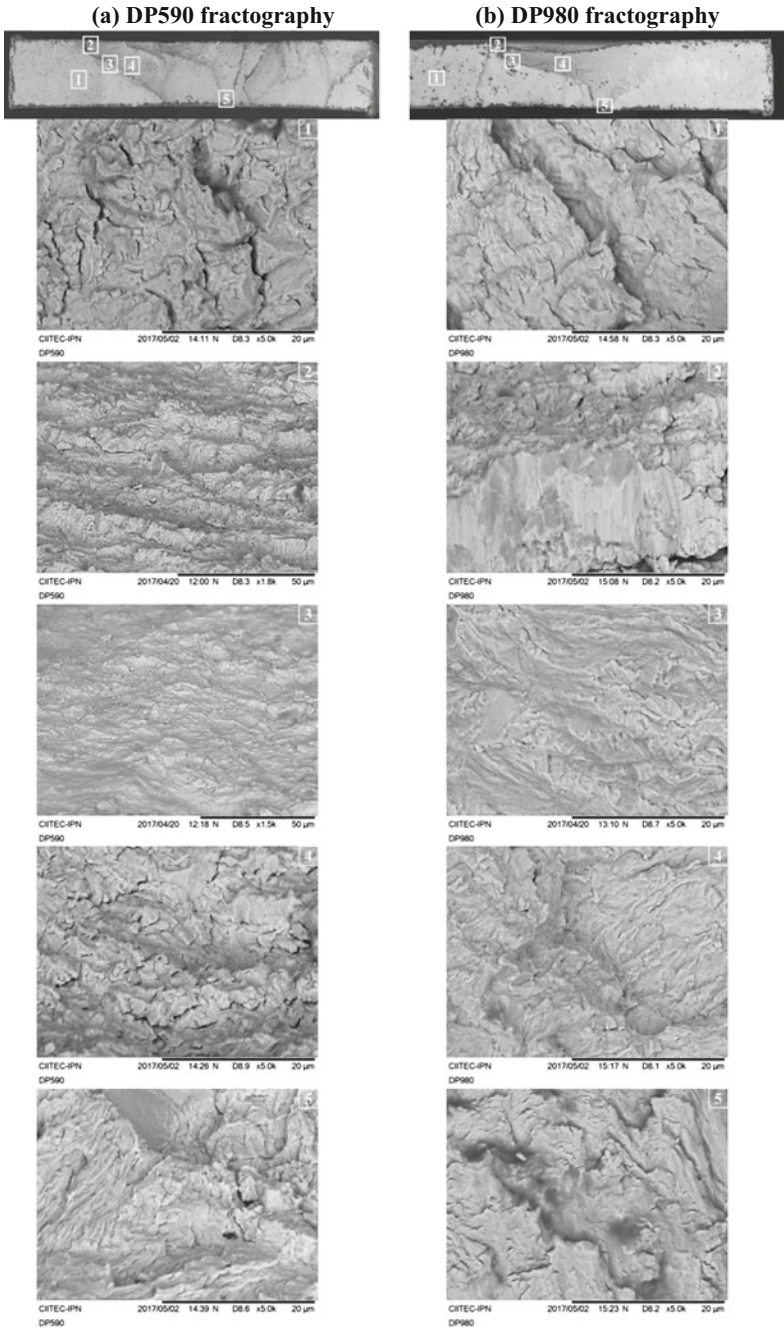
(a) DP590 fractography   **(b) DP980 fractography**

Fig. 8 Fracture surface appearance

Conclusions

The welding parameters have a great importance in the mechanical behavior of the resistance spot welds. The microstructural transformation in DP980 steel is higher severe than for the DP590 steel. This change was attributed to thermal input, which affects directly the mechanical properties of the material. In the case of DP980 steel a soft zone in the heat affected zone was detected, which is produced by the chemical composition of the material and the cooling thermal cycle of the resistance spot welding process. On the other hand, the tensile shear test shows a similar resistance in both steels, however, the displacement is higher than for the DP590 steel. It was observed that the stress concentration factor produced by the spot weld is the predominant aspect to decrease the fatigue resistance of the joints. A better fatigue behavior was observed for the DP590 steel.

References

1. S. Nayak, Y. Zhou, V. Baltazar Hernandez and E. Biro, "Resistance spot welding of dual-phase steels: heat affected zone softening and tensile properties," in *Proceedings of the 9th International Conference on Trends in Welding Research, Chicago, Illinois, United States*, 2012.
2. M. Pouranvari, "Susceptibility to interfacial failure mode in similar and dissimilar resistance spot welds of DP600 dual phase steel and low carbon steel during cross-tension and tensile-shear loading conditions," Materials Science and Engineering: A, vol. 546, pp. 129–138, 2012.
3. R. W. Rathbun, D. Matlock and J. Speer, "Fatigue behavior of spot welded high-strength sheet steels," Welding Journal, vol. 82, no. 8, pp. 207–218, 2003.
4. S. Dancette, D. Fabregue, V. Massardier, J. Merlin, T. Dupuy and M. Bouzekri, "Investigation of the tensile shear fracture of advanced high strength steel spot welds," Engineering Failure Analysis, vol. 25, pp. 112–122, 2012.
5. N. Farabi, D. Chen and Y. Zhou, "Microstructure and mechanical properties of laser welded dissimilar DP600/DP980 dual-phase steel joints," Journal of Alloys and Compounds, vol. 509, no. 3, pp. 982–989, 2011.
6. S. Mediratta, V. Ramaswamy and P. R. Rao, "Influence of ferrite-martensite microstructural morphology on the low cycle fatigue of a dual-phase steel," International journal of fatigue, vol. 7, no. 2, pp. 107–115, 1985.
7. S. K. Giri and D. Bhattacharjee, "Fatigue behavior of thin sheets of DP590 dual-phase steel," Journal of materials engineering and performance, vol. 21, no. 6, pp. 988–994, 2012.
8. A. Sherman and R. Davies, "The effect of martensite content on the fatigue of a dual-phase steel," International Journal of Fatigue, vol. 3, no. 1, pp. 36–40, 1981.
9. M. Xia, M. Kuntz, Z. Tian and Y. Zhou, "Failure study on laser welds of dual phase steel in formability testing," Science and Technology of Welding and Joining, vol. 13, no. 4, pp. 378–387, 2008.

10. M. Xia, N. Sreenivasan, S. Lawson, Y. Zhou and Z. Tian, "A comparative study of formability of diode laser welds in DP980 and HSLA steels," Journal of Engineering Materials and Technology, vol. 129, no. 3, pp. 446–452, 2007.

11. M. Xia, E. Biro, Z. Tian and Y. N. Zhou, "Effects of heat input and martensite on HAZ softening in laser welding of dual phase steels," ISIJ international, vol. 48, no. 6, pp. 809–814, 2008.

12. N. Chen, H.-P. Wang, B. E. Carlson, D. R. Sigler and M. Wang, "Fracture mechanisms of Al/steel resistance spot welds in lap shear test," Journal of Materials Processing Technology, vol. 243, pp. 347–354, 2017.

13. M. Marya, K. Wang, L. G. Hector and X. Gayden, "Tensile-shear forces and fracture modes in single and multiple weld specimens in dual-phase steels," Journal of Manufacturing Science and Engineering, vol. 128, no. 1, pp. 287–298, 2006.

14. A. Mittal, "Dual Phase steels," in Automotive Worldwide, 2017, p. 9.

15. W. Xu, D. Westerbaan, S. Nayak, D. Chen, F. Goodwin, E. Biro and Y. Zhou, "Microstructure and fatigue performance of single and multiple linear fiber laser welded DP980 dual-phase steel," Materials Science and Engineering: A, vol. 553, pp. 51–58, 2012.